TU Delft

Delft University of Technology

Document Version
Final published version

Licence
CC BY

Citation (APA)
Hornnes, V., Hendrikse, H., & Høyland, K. V. (2026). Deriving an ice strength coefficient from mean crushing loads and observations on low-speed ice–structure interaction. *Journal of Hydraulic Research*, *64*(1), 82-94. https://doi.org/10.1080/00221686.2025.2599247

Important note
To cite this publication, please use the final published version (if applicable).
Please check the document version above.

Copyright
In case the licence states “Dutch Copyright Act (Article 25fa)”, this publication was made available Green Open Access via the TU Delft Institutional Repository pursuant to Dutch Copyright Act (Article 25fa, the Taverne amendment). This provision does not affect copyright ownership.
Unless copyright is transferred by contract or statute, it remains with the copyright holder.

Sharing and reuse
Other than for strictly personal use, it is not permitted to download, forward or distribute the text or part of it, without the consent of the author(s) and/or copyright holder(s), unless the work is under an open content license such as Creative Commons.

Takedown policy
Please contact us and provide details if you believe this document breaches copyrights.
We will remove access to the work immediately and investigate your claim.

This work is downloaded from Delft University of Technology.

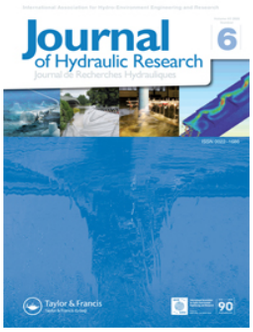

Journal of Hydraulic Research

ISSN: 0022-1686 (Print) 1814-2079 (Online) Journal homepage: www.tandfonline.com/journals/tjhr20

Deriving an ice strength coefficient from mean crushing loads and observations on low-speed ice–structure interaction

Vegard Hornnes, Hayo Hendrikse & Knut V. Høyland

To cite this article: Vegard Hornnes, Hayo Hendrikse & Knut V. Høyland (27 Jan 2026): Deriving an ice strength coefficient from mean crushing loads and observations on low-speed ice–structure interaction, Journal of Hydraulic Research, DOI: 10.1080/00221686.2025.2599247

To link to this article: https://doi.org/10.1080/00221686.2025.2599247

© 2026 The Author(s). Published by Informa UK Limited, trading as Taylor & Francis Group.

Published online: 27 Jan 2026.

Submit your article to this journal

Article views: 198

View related articles

View Crossmark data

Full Terms & Conditions of access and use can be found at
https://www.tandfonline.com/action/journalInformation?journalCode=tjhr20

JOURNAL OF HYDRAULIC RESEARCH
https://doi.org/10.1080/00221686.2025.2599247

IAHR AIRH International Association for Hydro-Environment Engineering and Research
Hosted by Spain Water and IWHR, China
Taylor & Francis Taylor & Francis Group

RESEARCH PAPER

OPEN ACCESS Check for updates

Deriving an ice strength coefficient from mean crushing loads and observations on low-speed ice–structure interaction

Vegard Hornnes [a], Hayo Hendrikse [b] and Knut V. Høyland[a,c]

[a]Department of Civil and Environmental Engineering, Norwegian University of Science and Technology, Trondheim, Norway; [b]Faculty of Civil Engineering and Geosciences, Delft University of Technology, Delft, The Netherlands; [c]The University Centre in Svalbard (UNIS), Longyearbyen, Norway

ABSTRACT

The design of flexible vertical offshore structures exposed to ice, like offshore wind turbines, can become governed by ice loads and structural responses at low relative ice speeds. This study attempts to quantify the low-speed ice loads based on a hypothesized interaction mechanism linking the velocity dependence of global loads to specific states of the ice supported by model- and full-scale observations. The quantified velocity effect is applied to estimate potential global pressures at low speeds from high-speed crushing events from the full-scale measurement campaign at the Norströmsgrund lighthouse. It is estimated that the velocity effect may produce global pressures equivalent to applying an ice strength coefficient of 0.9 MPa to 1.6 MPa. These results substantiate an alternative physics-informed approach to account for the velocity effect for ice loads and provide an interpretation of the interaction scenario captured by the 1.8 MPa value in the ISO19906 design standard.

ARTICLE HISTORY
Received 30 March 2025
Accepted 29 November 2025

KEYWORDS
Global ice loads; ice strength coefficient; ice–structure interaction; Norströmsgrund lighthouse; velocity effect

1. Introduction

The design of offshore structures in areas exposed to drifting ice must account for possible ice loads against the structure. For flexible vertical structures, such as offshore wind turbines, ice loads and the structural response associated with low relative speed between ice and structure can become governing for design. For deterministic design, the ISO19906 (2019) crushing equation is often used, which defines the characteristic design load as:

$$F_G = hwp_G \tag{1}$$

where F_G is the peak global ice load in continuous brittle crushing, h is the ice thickness, w is the projected structure width, or diameter in the case of a cylindrical structure, and p_G is the global ice pressure given by:

$$p_G = C_R\left[\left(\frac{h}{1}\right)^n\left(\frac{w}{h}\right)^m + f_{AR}\right] \tag{2}$$

with m an empirical coefficient equal to -0.16, n an empirical coefficient equal to $-0.5 + h/5$ for $h <$ 1.0 m, and -0.3 for $h \geq 1.0$ m, C_R an ice strength coefficient, and f_{AR} an empirical term given by:

$$f_{AR} = e^{\frac{-w}{3h}}\sqrt{1 + 5\frac{h}{w}} \tag{3}$$

Note that p_G, the global pressure, is the pressure averaged over the entire nominal contact area, and not the actual local pressure on the structure face. The crushing equation should remain valid for all ice drift speeds, and the ice strength coefficient C_R should incorporate the effects of factors such as natural variability of ice strength, duration of exposure of the structure to drifting sea ice, and ice drift speed (sometimes referred to as strain-rate). For the Baltic Sea a nominal value of 1.8 MPa is specified which is representative of a one-year maximum accounting for all those possible effects on the load, including effects of ice speed and structural compliance. The ice strength coefficient value is then to be combined with relevant return period ice thickness values in the crushing equation (ISO19906, 2019; Kärnä & Masterson, 2011).

In a discussion paper, Hendrikse and Owen (2023, p. 10) explored how the 'velocity effect', 'compliance effect' and 'dynamic amplification' are taken into account in the ice strength coefficient value of 1.8 MPa. Their analysis concluded that:

> When determining the design peak loads during intermittent crushing on the basis of the crushing equation in ISO19906, it is important that the C_R coefficient used accounts for the velocity effect. The velocity effect herein refers to the observation that level or pack ice loads are generally largest for low far-field ice drift speeds or low relative velocity between ice and structure. For the Baltic Sea region, the nominal value of 1.8 MPa contains a factor to account for this effect.

CONTACT Vegard Hornnes vegard.hornnes@ntnu.no

© 2026 The Author(s). Published by Informa UK Limited, trading as Taylor & Francis Group.
This is an Open Access article distributed under the terms of the Creative Commons Attribution License (http://creativecommons.org/licenses/by/4.0/), which permits unrestricted use, distribution, and reproduction in any medium, provided the original work is properly cited. The terms on which this article has been published allow the posting of the Accepted Manuscript in a repository by the author(s) or with their consent.

As explained by Kärnä and Masterson (2011, p. 8):

> the value $C_R = 1.8$ MPa was derived by applying a multiplying factor of 1.4 on the values that yield global pressures at the level of expected annual maximum

The factor was considered sufficient to account for effects from ice speed and structure compliance. Note that in their work, Hendrikse and Owen did not examine if the derivation of the C_R coefficient for the Baltic Sea was consistent with historical measurements of the velocity effect, considering the constant factor of 1.4 meant to account for the effect. This question becomes relevant when defining C_R values for the design of offshore wind turbines in the Baltic Sea. Current common approaches for this problem consist of using a subset of high-speed global crushing pressures measured at the Norströmsgrund lighthouse, fitting a statistical distribution to the pressures, and estimating what C_R values with certain return periods ought to be for a specific location with less or more ice exposure than the lighthouse (see, for example, Gravesen & Kärnä, 2009). Although these data only consist of high-speed loading events (though this is not explicitly mentioned in the report by Kärnä and Qu (2006), or in any derivative papers), this is typically either (1) not explicitly accounted for, or (2) accounted for by introducing additional 'velocity safety factors' or 'compliance effect factors'. These factors are either used as multipliers for C_R or included in advanced simulation models.

The above approach can lead to C_R values for design above 1.8 MPa and sometimes below 1.8 MPa. There are several challenges associated with this way of determining a value of C_R for design. The first challenge is the lack of transparency for the design load level due to the use of numerical models or structure dependent multiplication factors (accounting for the compliance effect), so the level of safety may vary from design to design. The second challenge is that there is no theoretical substantiation for the assumption that the exposure dependence of stochastic high speed crushing loads is like that of low-speed loads. Observations of intermittent crushing suggest limited dependence of peak loads on exposure, but the exact dependence is unknown. The third challenge is that the uncertainty associated with the data from the Norströmsgrund lighthouse, like that presented by Kärnä and Masterson (2011), are not taken into account. For example, the lighthouse was not fully covered by load panels, the panels only measured about 90% of the real load, and importantly the ice thickness measurements were not at the contact face and experienced high relative variability for the thinner ice.

Despite these challenges, there are reasons for working with the high-speed crushing data from the Norströmsgrund lighthouse. There are very few recordings of events classified as low speed synchronized loading on the lighthouse, thus little data to work with. In addition, low speed synchronized loads measured at the lighthouse were often not much higher than the high-speed brittle crushing loads. This can be explained by the relative rigidity of the structure, as is done in Section 3. Therefore, the more available recordings of high-speed stationary crushing were used to establish an ice strength coefficient value for design, and later a multiplying factor of 1.4 was added to account for what was not measured, arriving at 1.8 MPa for the Bay of Bothnia in ISO19906 (Kärnä & Masterson, 2011).

In this work, the data from the Norströmsgrund lighthouse is interpreted in a framework that can explain both high-speed and low-speed loading effects, the velocity effect, and the development of ice-induced vibrations on flexible structures. In this paper we attempt this seemingly novel step based on recent research on model-scale ice-structure interaction (Owen et al., 2023) and the conceptual framework behind the ice model by Hendrikse and Nord (2019). In the framework developed in the past decade, the velocity effect reflects intrinsic ice deformation and failure behaviour which can be observed on any structure, whether rigid or flexible, provided the relative velocity between ice and structure is sufficiently low for a sufficiently long time. As such, all structures could experience synchronization of pressures and/or contact area increase across their circumference during events with low-speed loading (such as ice stopping against a structure), but the degree of synchronization depends on how long the low speed is maintained. The increase in contact area and synchronization of contact pressure for low-speed events was also seen in the tests described by Sodhi et al. (1998). If the conceptual framework is indeed a correct representation of reality at the level of global loads, very flexible structures can move with the ice, thereby reducing the relative velocity between the ice and structure. This allows the ice to 'strengthen' through spatial pressure synchronization and/or contact smoothening. Rigid structures on the other hand require more specific ice velocities to observe the same effect, such as when ice floes come to a very gradual stop. We use the term 'conceptual framework' here to highlight that despite the ability of models based on these concepts to capture many model- and full-scale observations, we do not provide a full physical description of the complicated mechanics involved in ice crushing and dynamic ice–structure interaction and there is no explanation of what physically happens locally in the ice during the interaction.

In this paper, we reanalyse the Norströmsgrund lighthouse data based on the above-mentioned conceptual framework of pressure/area synchronization and effect of relative velocity. Based on the framework, we estimate the pressure ratio between low-speed peak pressures compared to high-speed mean pressures, observed from other low-speed ice–structure interaction events in model- and full-scale. We then apply the ratio to high-speed events at the lighthouse,

Table 1. List of high-speed ice brittle crushing events selected for further analysis. Modified from Hornnes et al. (2024).

Date	Time start	Time stop	Mean load (kN)	Mean pressure (kPa)	Peak pressure (kPa)	Mean thickness (m)	Drift direction (°)
3 March 2000	17:50:00	18:08:20	875	409	833	0.30	90
3 March 2000	18:35:00	18:40:00	753	381	628	0.28	90
3 March 2000	19:15:30	19:18:30	725	317	503	0.32	90
3 March 2000	20:23:04	20:54:51	840	263	443	0.45	90
21 March 2002	20:20:30	20:23:00	1336	265	473	0.73	45
19 March 2003	21:54:20	21:55:45	1739	292	451	0.86	45
19 March 2003	21:56:55	21:57:55	1144	304	525	0.54	45

to estimate the peak low-speed pressures that could occur for the same ice conditions (ice thickness and physical properties). The low-speed peak pressures are compared to different values of the ice strength coefficient C_R. The comparison indicates the severity of the estimated low-speed peak pressures compared to recommended design values at the location, and the level of pressure synchronization that is reflected in different values of C_R.

This method represents a shift in approach in the way the velocity effect is accounted for when defining possible peak global pressures. To derive the ice strength coefficient value of 1.8 MPa, Kärnä and Masterson (2011) accounted for ice speed and structure compliance by applying a constant factor of 1.4 to peak pressures at the level of annual maximum. In contrast, we attempt to use a physics-informed approach along with observations of the velocity effect in model- and full-scale to define possible peak global pressures. Instead of treating peak pressure values as statistical extreme values multiplied with a factor, we consider the type of interaction (i.e. a pressure synchronization at low speed) that could result in the peak pressure values, and the range of pressures that might be expected to occur during such an interaction. This type of interaction behaves differently from the high-speed crushing used to derive statistical extreme values and will likely have different dependence on factors like exposure or duration of loading.

In Section 2 of this paper the full-scale data used in this paper is introduced, the methods used for the data reanalysis are explained, and the selection criteria for the events are presented for reproducibility. Section 3 introduces the conceptual framework and defines the ratio of the maximum low speed load to the mean load during high-speed crushing as a critical parameter based on model-scale and full-scale observations. In Section 4 this ratio is used in combination with high-speed mean global crushing pressures measured at the lighthouse to determine the range of low-speed global pressures that could have developed in the same ice conditions at a low interaction speed. These results are compared to the ice strength coefficient of 1.8 MPa as suggested in ISO19906 and discussed in the final section. This paper is based on and extends the conference paper "Establishing the ice strength coefficient from mean crushing loads and a theoretical velocity effect", presented at the IAHR conference "27th IAHR International Symposium on Ice" in Gdańsk, Poland, 2024 (Hornnes et al., 2024). This work extends the analysis to the individual load panel data, expands on the applied conceptual framework, and further investigates the effect of ice thickness variability and ice exposure length on the loads and pressures.

2. Norströmsgrund lighthouse data

In the winters from 1999 to 2003, full-scale ice-structure interaction data were recorded as a part of the Validation of Low Level Ice Forces (LOLEIF) and Measurements on Structures in Ice (STRICE) campaigns at the lighthouse Norströmsgrund, located in the Bay of Bothnia (Bjerkås, 2006; Schwarz & Jochmann, 2001). The data was reanalysed following a similar methodology as in Hornnes et al. (2024) to establish global loads and pressures, outlined in the current section. Simultaneous load and environmental data recorded during the LOLEIF and STRICE campaigns were collated and cleaned of errors. Like in Hornnes et al. (2020), the recorded environmental data were interpolated to 1 Hz using a previous neighbour interpolation routine. Further, to establish high-speed brittle crushing events for analysis, the following selection criteria were applied to the time series:

- there is interpolated ice thickness data, and the thickness is greater than 0.1 m;
- there is interpolated ice velocity data, and the ice speed is greater than 0 m s^{-1}. Alternatively, the approximate velocity at the time could be substantiated from reports, video recordings, or logged observations made at the lighthouse;
- the angle of approach is between 45° and 90°, corresponding to ice approaching from between northeast and east, to be confident that most of the global load is captured; and
- local load panel loads are available.

Applying these selection criteria reduced the dataset to a total of 75 time series. Further, we found the global load by projecting the load on each load panel onto the reported ice drift direction and taking the sum. The load components orthogonal to the reported ice drift direction were not included in the global load. We increased the loads by 10% of the measured values based on the load panel calibration report (Fransson,

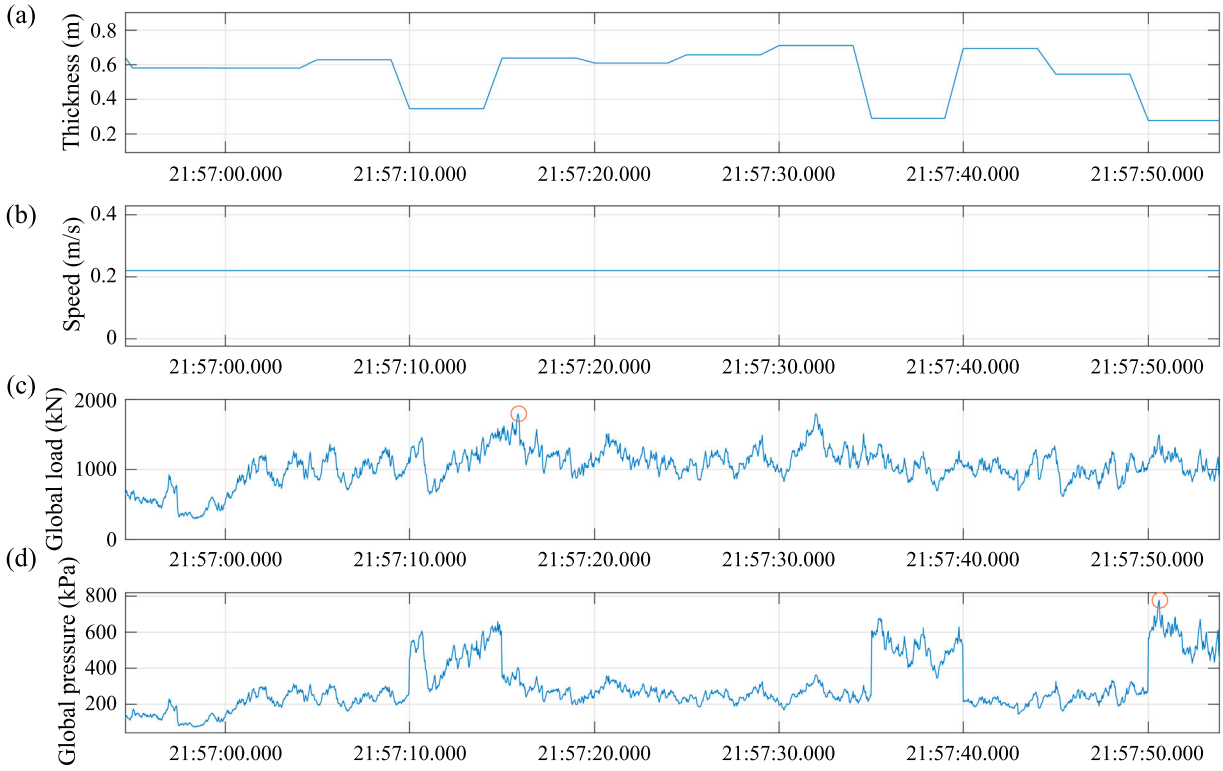

Figure 1. (a) The ice thickness, (b) speed, (c) global load and (d) global pressure time series for the final event in Table 1. The global pressure shown is calculated from the simultaneously occurring global load and ice thickness. The peak load and peak pressure are marked with red circles in the respective time series. Adapted from Hornnes et al. (2024).

2001). Then, we did a visual inspection of the time series and accompanying footage to find stationary brittle crushing or ice stopping after crushing. For crushing events, we applied the requirements that there is at least one minute of continuous crushing without large fluctuations in mean global load, loads should not drop to zero, there is no obvious thick ice inclusions or open water, and loads should not drop below 50 kN during the crushing for at least seven panels. The resulting brittle crushing events are listed in Table 1, and the time series for one such event is shown in Figure 1.

Due to the large relative uncertainty in ice thickness compared to the uncertainty in load, in particular for events with thinner ice, the peak global pressure during each brittle crushing event will often be found at the point in time that happens to have the lowest ice thickness measurement, as illustrated by red circles in Figure 1. Thus, the peak pressure can potentially be exaggerated when the crushing event is too short. There is no immediate connection between the ice thickness and the load measured at the same point in time, due to the 6–10 m distance between the thickness measurement and the load panels and due to the spatial variability of ice thickness across the load panels. Hence, calculating the instantaneous pressure based on the simultaneously occurring thickness measurement will not necessarily be accurate. Therefore, the mean thickness was used to calculate pressures, and the peak global pressure $p_{\max,BC}$ during brittle crushing was found as:

$$p_{\max,BC} = \frac{F_{\max,BC}}{h_\mu w_p} \tag{4}$$

where $F_{\max,BC}$ is the peak global load during each brittle crushing event, w_p is the projected width of the structure covered by load panels in the ice drift direction, and h_μ is the mean measured ice thickness during each crushing event. The projected width was 6.94 m and 7.18 m for drift directions of 45° (north-east) and 90° (east) respectively, due to the placements of the load panels. The mean global ice pressure $p_{\mu,BC}$ during each brittle crushing event was found as:

$$p_{\mu,BC} = \frac{F_{\mu,BC}}{h_\mu w_p} \tag{5}$$

where $F_{\mu,BC}$ is the mean global load during the crushing event. In addition to the methodology used in Hornnes et al. (2024) to find global loads and pressures, the individual panel pressures during brittle crushing were analysed. The mean and peak pressures on each panel during brittle crushing was calculated similarly as the global pressures, except for using a panel width of 1.2 m instead of the projected width of the entire structure.

Several sources of additional uncertainty were present in the data:

- The ice thickness was measured by a combination of methods 6–10 meters from the lighthouse for different years. Due to the distance and measurement methods, the measurements do not give the simultaneous ice thickness at peak load. Also, as the ice thickness measurements were often found to vary at the metre scale (length) by about ±0.05 m during crushing, the thickness was never the same over

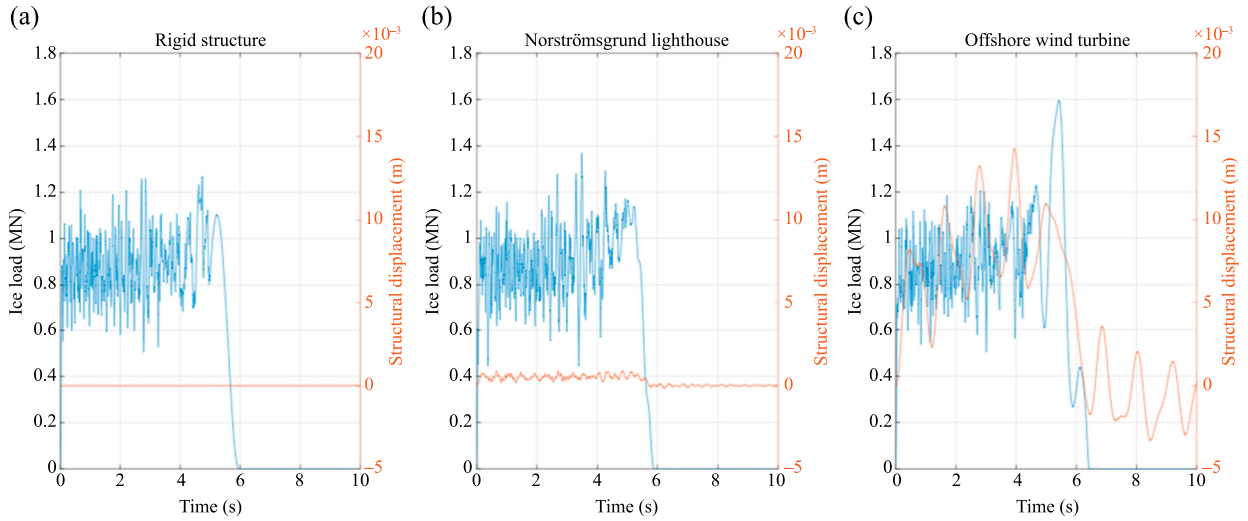

Figure 2. Examples of simulations of an ice floe stopping against (a) a completely rigid structure, (b) a model of the Norströmsgrund lighthouse, and (c) a flexible wind turbine. Simulations were made with the model developed by Hendrikse and Nord (2019). Adapted from Hornnes et al. (2024).

the entire circumference of the lighthouse. The variability in the ice thickness measurements can result in uncertainty in estimated properties such as peak pressure, and for instance when plotting peak pressures against ice thickness. For 0.3 m ice thickness the uncertainty in peak pressure can be up to 25%. Estimating the mean global pressures from the mean thickness during an event is expected to decrease the variability. However, there will still be underlying inaccuracy in the estimated global pressures due to the above-mentioned features of the ice thickness measurements.

- Measurements of drift directions were just as rare as ice speed measurements, and sometimes did not correspond with the loaded panels. The panel loads were projected onto the drift direction and may have been affected by inaccuracies in the direction. Additionally, the pressure calculation may have been off by at most 20% if less contact could be accounted for, such that the projected width became incorrect.
- We did not have data from all directions for entire seasons, which means we could not judge to what degree the specific events found are representative of annual maxima.

3. Low-speed spatial pressure synchronization and full-scale observations of the velocity effect

Relevant aspects of the framework we adopted for low-speed spatial pressure synchronization are introduced in Section 3.1. In Section 3.2, full-scale observations of the velocity effect are introduced to substantiate a range of values for the ratio between the maximum synchronized load at low ice drift speed and the mean brittle crushing load at high drift speed.

3.1. Conceptual framework

The conceptual framework adopted here assumes, as found in model-scale experiments and assumed equally applicable to full-scale, that ice loads on a rigid structure are largest at a low speed where the failure mode transitions from ductile to brittle (Owen et al., 2023; Sodhi et al., 1998). Note that this concerns only the global loads experienced by the structure, as it has also been shown that local pressures can be higher at high speed compared to low speed (Sodhi et al., 1998). The fact that these local pressures at high speed do not occur simultaneously over the entire contact area means these do not lead to larger global loads. An exception to this statement would be when the size of the structure is very small, as in that case the area of local pressure may become equal or close to the global contact area. The latter is often not the case for offshore structures of interest here.

This effect of an increased global load at low speed can be interpreted as a 'strengthening' of the ice, where the term 'strengthening' is loosely applied to describe the observations of a higher load at ice failure. The term encompasses the effects of both a potential increase in contact area and redistribution of pressure, as the local mechanism responsible for the rapid increase in load remains unknown. The effect is observed when the relative velocity between the ice and the structure remains low for sufficiently long, such as during intermittent crushing.

When a flexible structure is interacting with ice, the motion causes the relative velocity to vary and sometimes reduce to the range where this rapid load increase can develop. If this happens, ice-induced vibration regimes such as intermittent crushing and frequency lock-in can develop, with high peak ice loads associated with them. Consequently, high loads are observed more

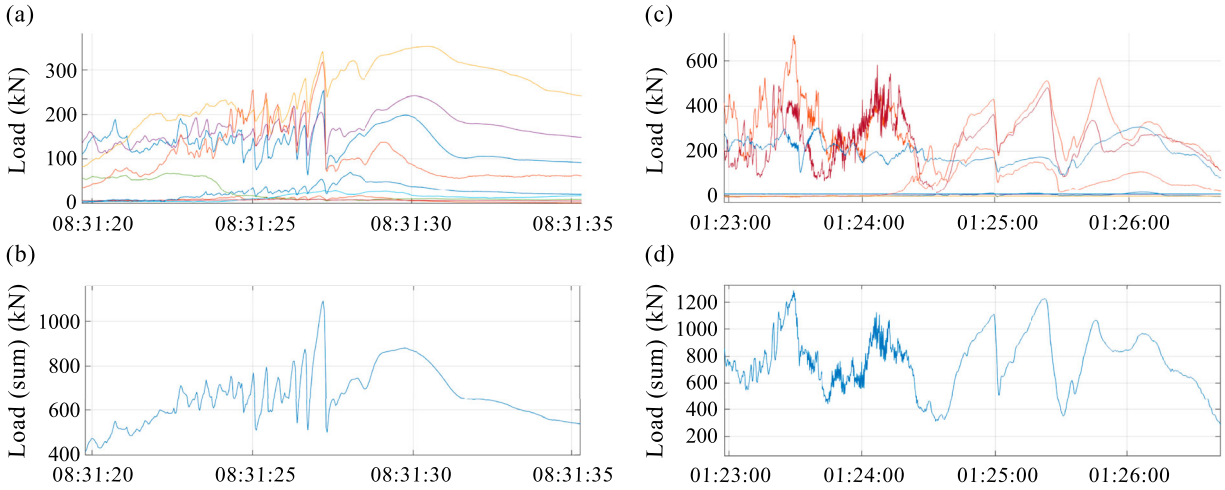

Figure 3. Two instances of ice load synchronization against the Norströmsgrund lighthouse, shown from panel loads (a) and (c), and global load (b) and (d). The stopping event shown in (c) and (d) has limited panel coverage, but transitions through several interaction modes before the load becomes static. Adapted from Hornnes et al. (2024).

frequently on flexible structures as there are more conditions leading to low relative velocities when compared to rigid structures. This has in literature been referred to as the 'compliance effect'. It should not be mistaken for the statement that the maximum loads a specific ice sheet can exert on flexible structures are larger than on rigid structures.

An important conclusion when adopting this concept is that relatively rigid structures in nature are not great measurement devices to capture the potentially largest ice loads. For rigid structures there is only a small range of ice speeds for which any low-speed 'strengthening' can be observed (the existing data, as introduced below, suggests in the order of 1 mm s^{-1} to 10 mm s^{-1}). Naturally occurring ice drift with such constant low speeds does not occur often or requires very specific driving forces. The effect could, for example, be observed for ice floes slowing down and coming to a stop due to insufficient driving forces. But in that case it requires the stop to be very gradual, or there is simply insufficient time for the synchronization to fully develop.

A simulated example for illustration purposes is shown in Figure 2, using the model developed by Hendrikse and Nord (2019), where flexible and more rigid structures are compared in the same ice conditions. The rigid structure data seen in Figure 2a suggests the peak loads develop at high speed during continuous crushing, but the potential of the ice is only observed in Figure 2c for the flexible structure where the structural motion causes the relative velocity to remain small for a longer time and a load increase of 30% develops right before the ice floe comes to a stop.

Note that the framework discussed here only focuses on understanding the ice load as it is affected by ice velocity and motion of the structure caused by structure compliance. Many other factors will influence the ice load on a structure, including ice properties (for example temperature, salinity, density), existing flaws and cracks, as well as the ice microstructure (ISO 19906, 2019). These latter factors are not explicitly accounted for. Lastly, it is often observed that during intermittent crushing the loads typically drop down to the mean high-speed brittle crushing load right after failure and at the start of a new loading cycle. Sometimes this is interrupted by zero loads due to contact loss, but after re-establishing the contact the load level appears to be around the high-speed mean brittle crushing load again. Examples can be observed in the tests reported by Kärnä and Muhonen (1990) and by van den Berg et al. (2022). This is explained by the short period of high relative velocity between ice and structure developing after a moment of failure, which effectively causes a short period of continuous brittle crushing. This effect can be used to determine a typical ratio of low-speed maximum load to high-speed mean load from full-scale observations, which is done in the next section. The ratio then enables the use of high-speed mean loads obtained from rigid structures for estimating the maximum loads the ice could put on the structure at low speed, provided the spread in observed ratios in different model-scale and full-scale measurements is limited.

3.2. Ratios of the low-speed maximum load to the high-speed mean brittle crushing load

Here we present full-scale data and estimate typical ratios of the mean high-speed brittle crushing load and measured low-speed peak loads. The ratio of peak loads to mean brittle crushing load is shown in Table 2. The best examples are found for ice floe stopping events, such as the Molikpaq 12 May 1986 event (Gagnon, 2012). Data from the Norströmsgrund lighthouse are shown in Figure 3. As described in Section 3.2, observations of intermittent crushing could also be used to

Table 2. Ratios of maximum low-speed load to mean brittle crushing load estimated from model-scale and full-scale data. Adapted from Hornnes et al. (2024).

Source	Ratio	Note
Cook Inlet (Peyton, 1968)	~ 4	Ice floe slowing down against a Cook Inlet test pile.
Molikpaq (Gagnon, 2012)	~ 2	Ice floe slowing down against the Molikpaq. The piece of ice breaking off at around 24 min may cause the mean high-speed load to be somewhat overestimated. This factor is therefore considered a lower estimate.
Norströmsgrund (this paper, Figure 3)	~ 1.7	This is a relatively low ratio, but the stopping event is relatively quick. The structure is quite rigid, meaning the true potential load increase may not develop as illustrated in Figure 2.
Norströmsgrund (Schwarz & Jochmann, 2001)	~ 3	A startup event with partial panel coverage illustrating how the loads on the lighthouse can increase to high values after a period of very slow loading.
Model-scale at Aalto Ice and Wave Tank (Owen et al., 2023)	~ 3–4	The final peak load is very high due to a very small deceleration (very slow stop).
Model-scale Iowa (Hirayama et al., 1973)	~ 1.7	An example of intermittent crushing where the final load peak reaches a ratio of 2.3. The ratio of 1.7 is a lower bound estimate of what is possible for the given conditions.
Model-scale CRREL (Sodhi, 2001)	~ 4	Intermittent crushing from experimental campaigns.

estimate this ratio. This data can be amended with model-scale experiments where intermittent crushing was observed such as by Hirayama et al. (1973) and Sodhi (2001).

Note that larger ratios between low-speed peak loads and mean high-speed crushing loads than those mentioned in Table 2 have been observed in conditions where the initial contact is with a prepared ice surface. Examples can be found in Croasdale (1977) and Sodhi et al. (1998), where the initial load peak is 5–6 times higher than the following high-speed mean, which the authors attribute to the large simultaneous ice–indentor contact area. This state provides an upper bound estimate for the ratio under investigation here. However, a condition of full-thickness, full-width contact is unlikely to occur in nature when drifting sea ice interacts with an offshore structure, especially in the case of cylindrical structures. Full-thickness contact is therefore considered less relevant than the contact with a wedge-shaped front of an ice sheet developed due to prior crushing failure or interaction with the structure.

4. Estimating the potential low-speed synchronized loads based on mean high-speed crushing loads

Based on the data presented in Section 3.2, a factor 3–4 times the high-speed mean brittle crushing load is assumed to give a good indication of what the peak loads in certain conditions might be if the velocity becomes low for sufficiently long to fully activate the velocity effect (e.g. obtain full spatial pressure synchronization/smoothened contact). In Figure 4a we apply these factors to the high-speed brittle crushing pressures found for the global load events in Table 1, to estimate the low speed synchronized peak pressures. Considering all the events, the estimated synchronized global pressures range from about 0.8 to 1.6 MPa, depending on ice thickness. The highest global pressures occurred for the thinnest ice, but any trend of decreasing pressure with thickness is less clear above 0.4 m. The peak global pressures measured during high-speed crushing ranged from 1.5–2 times the mean pressures for each event, meaning that the estimated synchronized pressures are well above the peak high-speed crushing pressures. This is as expected, as the probability of significant pressure synchronization or a 'perfect' contact between ice and structure during high-speed brittle crushing is relatively low. From the few events considered here, no correlation could be observed between the event duration and relative pressure peak magnitude.

In Figure 4b, the mean and peak panel pressures for the nine load panels for each crushing event are shown. Compared to the global pressures, the peak panel pressures during high-speed crushing were significantly higher, as the panel widths were only about 16% of the structural width for which the probability of a significant pressure synchronization or a 'perfect' contact between ice and structure during high-speed crushing is inherently higher than when considering the whole structure. In comparison, the mean panel pressures were closer to the mean global pressures, which is expected during brittle crushing.

For comparison purposes, the estimated synchronized global pressure ranges from Figure 4a are also included in Figure 4b. As was seen in the segmented indentor tests by Kamesaki et al. (1996), it is expected that peak panel pressures would remain similar for synchronized failures at low ice drift speed, as for non-synchronized failures at higher ice drift speed. Because the failures synchronize at low ice speed, the peak panel pressures during crushing should be closer to the synchronized global pressure on the lighthouse. In Figure 4b it is seen that the largest panel pressures are in the range of the estimated synchronized peak global pressures. To some degree, this supports the assumption that 3–4 times the mean global crushing pressure gives an indication of the potential synchronized global pressure, given the same ice conditions.

Finally, the estimated synchronized peak global pressures were compared against assumptions for ice strength coefficients in the context of structural design. In Figure 5, the synchronized peak global pressure ranges are compared with global pressures as found from Equation (2) for different values of C_R, assuming a

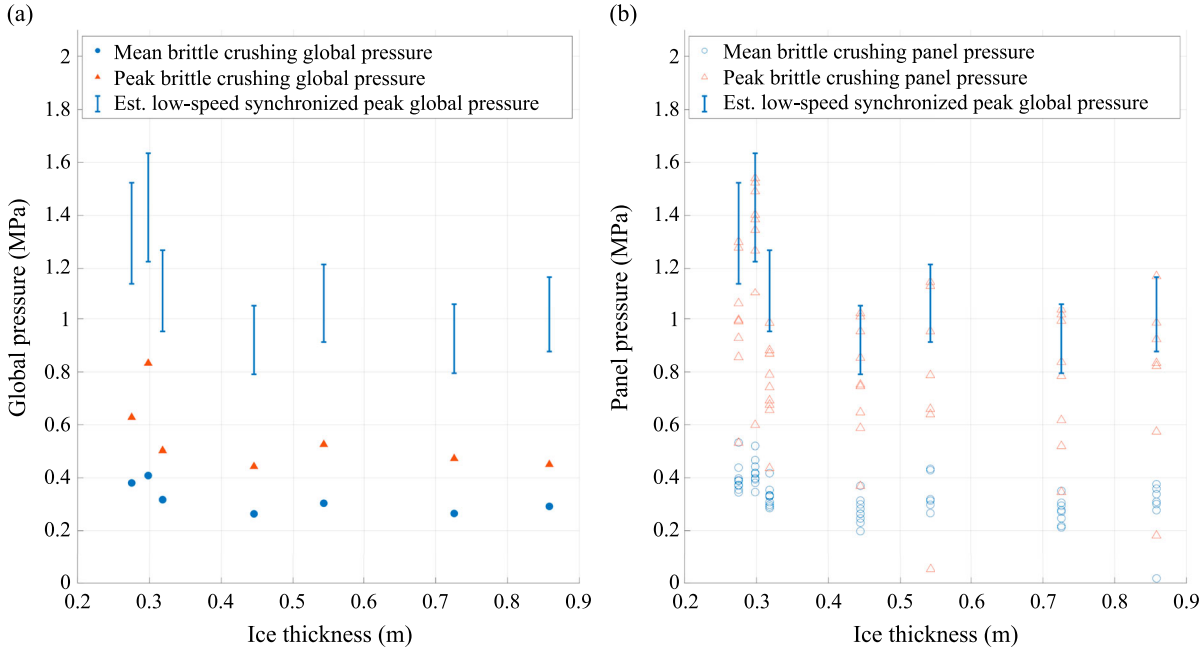

Figure 4. (a) Mean (blue round points) and peak (red triangles) global pressures versus ice thickness for high-speed brittle crushing events at Norströmsgrund given in Table 1. The blue, vertical lines above each point show the range 3–4 times mean global pressures. (b) Mean (blue circles) and peak (red unfilled triangles) pressures for individual load panels versus ice thickness for high-speed brittle crushing events at Norströmsgrund are given in Table 1. The blue, vertical lines show the same 3–4 times mean global pressure range as in (a).

structural width of 7.58 m. Depending on the assumed degree of synchronization, low speed loads are expected to be possible in the range from (expressed in C_R) 0.9 to 1.6 MPa, provided crushing is expected to develop. For very severe static events higher values may be expected. Note that we do not know how representative the mean pressures shown here are for all events that occurred at the lighthouse, as it could be that our selection criteria have resulted in only selecting 'weak' or 'strong' ice. However, the associated peak global pressures in Figure 5 are similar to those reported by Kärnä and Masterson (2011).

5. Discussion

This study proved to be more complicated to carry out than originally expected. The events and methods used to find the global pressure values at the Norströmsgrund lighthouse and reported by Kärnä and Masterson (2011) were not found in the original report by Kärnä and Qu (2006) that the authors cited. Thus, the original dataset had to be reanalysed to find brittle crushing events with relatively certain environmental data (ice thickness, velocity) and load panel loads. Applying our reqirements, only seven time series resulted from the analysis, which may be attributed to:

- Our requirements being stringent, especially in terms of environmental data.
- Selection of events. To reduce uncertainty in the mean pressure, we preferred longer events of brittle crushing wherever possible, while selecting shorter sub-events could have resulted in more events. Some events with significantly weaker pressures than other events at equivalent ice thickness were also not included.

Selecting sub-events which happened to have low, simultaneously measured ice thickness could artificially 'inflate' the peak pressures. Additionally, the large uncertainty in the ice thickness measurement would propagate to both the calculated pressures as well as the estimated synchronized peak global pressure. To illustrate this, the longest crushing event (the fourth event in Table 1) was sub-sampled into six sub-events of approximately equal durations of about 5 min 20 s each. Figure 6a shows the mean, peak, and synchronized pressure range for each sub-event, while curves of Equation (2) for two values of C_R are included for comparison. While the mean loads for the sub-events ranged from 700 to 800 kN, the relatively large range in ice thickness was the primary source of variability in both mean pressures and the estimated synchronized peak pressures. This is further illustrated in Figure 6b, where the mean, peak, and synchronized global pressure range at the bounds of the observed ice thickness variability of ± 0.05 m is shown for the same event as in Figure 6a. Any inaccuracy or errors in the ice thickness will be multiplied by 3–4 as it propagates to the synchronized global pressure, which would affect events with the highest mean crushing pressures to a greater degree. The true inaccuracy in the ice thickness measurements are unknown, but the sub-sampling and pressure range due to ice thickness variability illustrates the significant

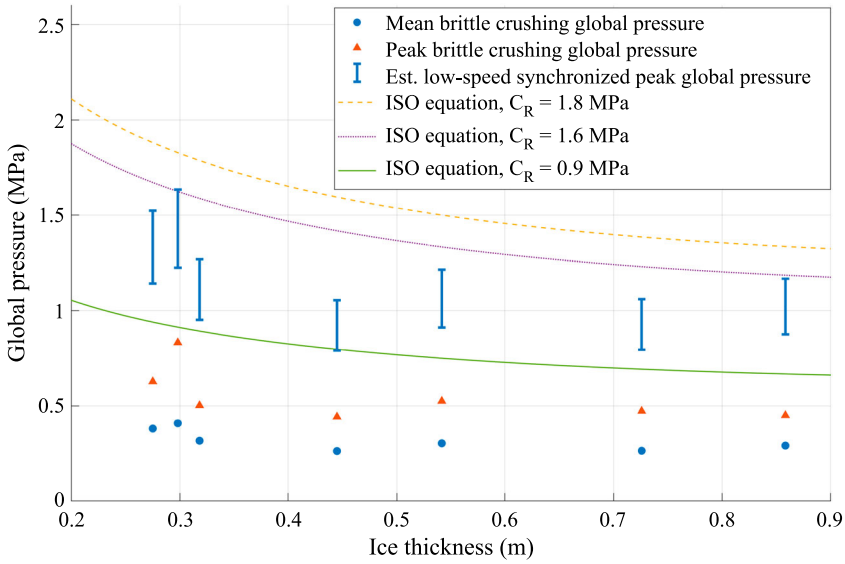

Figure 5. A comparison of the estimated low-speed synchronized peak global pressures (shown as blue, vertical lines) and global pressures from Equation (2) for different values of C_R (shown as curves). The mean (blue, round points) and peak (red triangles) show global pressures as a function of ice thickness for high-speed brittle crushing events at Norströmsgrund as given in Table 1. Modified from Hornnes et al. (2024).

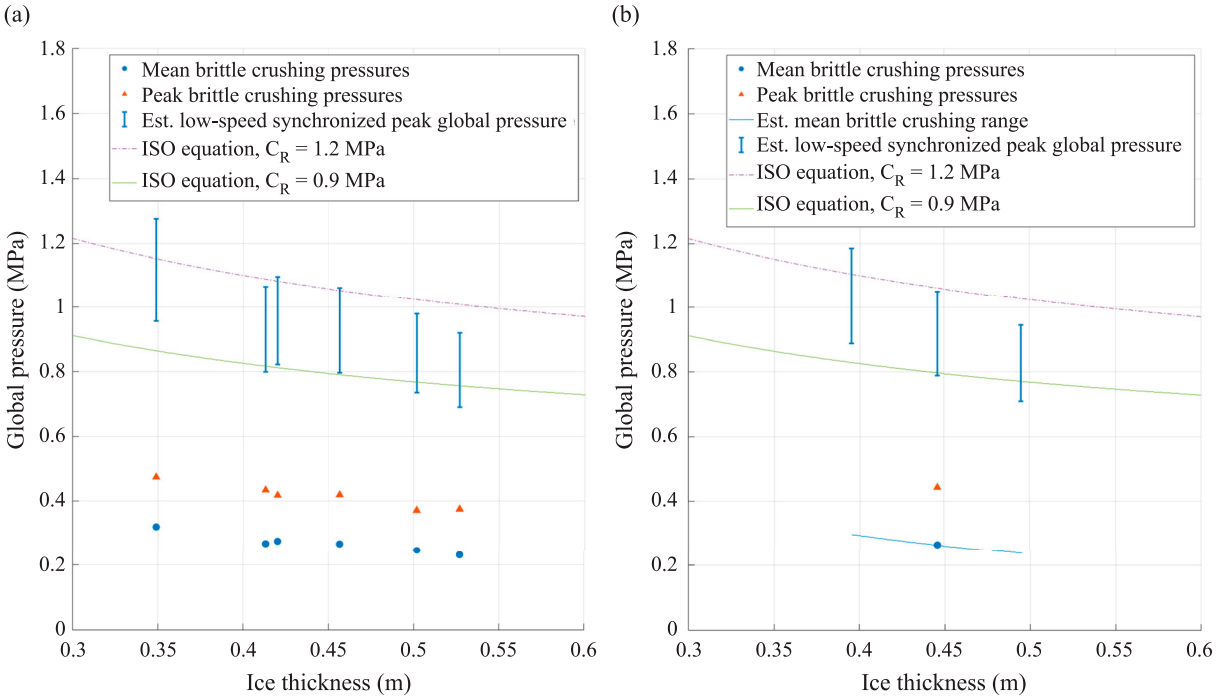

Figure 6. Mean (blue round points) and peak (red triangles) global pressures along with the resulting estimated synchronized pressures shown as blue, vertical lines. (a) Sub-divisions of the longest crushing event in Table 1. (b) The estimated mean pressure range (blue line intersecting the mean pressure point) based on ±0.05 m ice thickness variability, along with the resulting estimated synchronized pressures for the minimum and maximum mean pressure. Curves showing Equation (2) for two values of C_R are included for reference.

degree of uncertainty associated with plots like Figure 5, and the need to account for that uncertainty when using them as a basis for design.

An interesting lock-in event was noted during the reanalysis, with mean pressure of 0.470 MPa and peak pressure of 0.963 MPa at 0.71 m mean ice thickness. Compared to the brittle crushing event at a mean ice thickness of 0.73 m shown in Figure 5, the mean and peak global pressures during the lock-in event are approximately 77% and 100% higher, respectively. The event has previously been mentioned in literature, in the context of its high global load for being level ice (event 28 in Ervik et al., 2019) and the large acceleration it imposed on the lighthouse (event 55 in Nord et al., 2018). The event itself (Figure 7) may have contained significant pressure synchronization and is a good example of a type of event that must be captured by the ice strength coefficient used for design

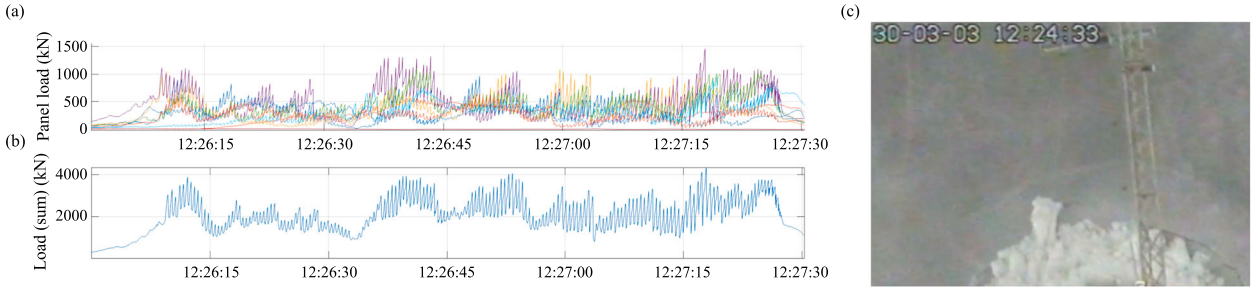

Figure 7. (a, b) The load-time series of a lock-in event at the lighthouse, which occurred 30 March 2003 from 12:26:10 to 12:27:25. (c) An image of the surveillance video from the lighthouse showing circumferential cracks appearing before the leading edge hits the structure and lock-in occurs. Adapted from Hornnes et al. (2024).

purposes. The interaction seems to start after formation of a circumferential crack, which may have prepared the surface resulting in good contact between the incoming ice sheet and structure.

During the analysis, we found indications of synchronized load increases (Figure 3) and lock-in (Figure 7), which all yielded relatively high loads and pressures in their respective time series. As such, the lighthouse behaved fairly rigid, but not fully rigid under high loading and thick ice which could sustain the loading. The rigidity did however mean that the lighthouse might not have experienced the maximum force that could potentially develop during most interactions with ice. Thus, there is the risk that statistical methods based only on this dataset may inherently underpredict the maximum load that could develop.

Compared to our analysis, the 1-year nominal value of 1.8 MPa intended to capture effects of ice speed and structure compliance (Kärnä & Masterson, 2011) is on the high side, and therefore may be a good choice when considering its use for design and the need to have a safe estimate. The value of 1.8 MPa lies in the range of 5–6 times the mean global crushing pressure. The magnitude of this increase does mirror observations from full-scale tests with perfect full-thickness initial contact between ice and structure (Croasdale, 1977; Sodhi et al., 1998), which could be a scenario considered in the definition of the value of 1.8 MPa. Still, despite the difference in approach in this study and that of Kärnä and Masterson (2011) to account for the velocity effect, the similarity to the 1.6 MPa value may substantiate this method of accounting for the velocity effect in defining ice strength coefficient values. Note also that the 1.6 MPa value results from multiplying the largest mean crushing pressures found in this work by four. Higher mean crushing pressures would result in a higher low-speed peak estimate, but due to the lack of data the probability of higher mean pressures is unknown.

The 1-year value of 1.34 MPa as mentioned in the ISO19906 (2019), using the 135 km ice distance travelled proposed by Thijssen and Fuglem (2015), falls in the range of three to four times the mean crushing pressure due to synchronization as estimated here. The value is on the higher end of what has been observed for stopping events and intermittent crushing in the full-scale and model-scale events we analysed. The 1-year value of around 0.75 MPa for the Bay of Bothnia by Gravesen and Kärnä (2009) reflects a factor approximately two times the high-speed mean crushing pressure, which significantly underestimates the expected pressure for synchronized loading at low speed on rigid structures. Gravesen and Kärnä do propose to increase this value to account for compliance of the structure, which means inherently accounting for a lower probability of sufficiently low ice speed conditions on a rigid structure. For a very compliant structure this value would increase to 1.5 MPa, which would be in the upper range of four times the mean global crushing pressure consistent with our analysis.

Based on our analysis, values below 0.9 MPa for the ice strength coefficient reflecting a 1-year maximum value in any location in the Baltic may not sufficiently account for spatial pressure synchronization at low relative speed. A value lower than 0.9 MPa representative of a 1-year maximum ice strength coefficient could theoretically be justified for a rigid structure if one could find a way to account for the actual probability of having sustained low-speed loading.

In this study, we compare mean and peak high-speed crushing loads, as well as peak low-speed loads. While it is expected that these parameters share some dependence on ice properties such as temperature, salinity and thickness, there is also a clear difference in the expected dependence on exposure, or duration of loading. The high-speed maximum crushing load will depend significantly on the duration of loading, with the probability of having several high-speed local pressure spots developing simultaneously increasing with increased duration of loading. The mean high-speed load, however, is expected to show less dependence on duration of loading, or exposure, as it reflects the average high-pressure zones in contact with and simultaneously pushing the structure. For low-speed maximum loads there are indications that the effect of exposure is smaller than what is observed at high-speed, but the exact dependence is unknown. An example can be observed in relatively stable intermittent crushing load

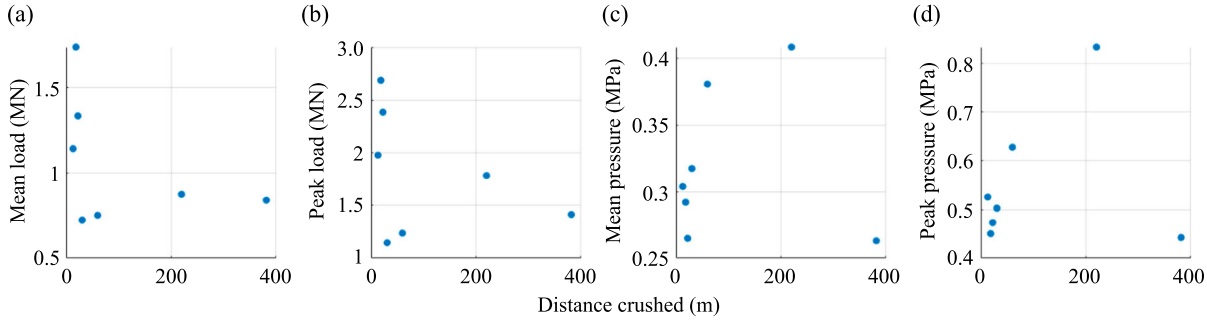

Figure 8. Ice distance crushed during each event in Table 1, estimated from ice speed and event duration, versus mean and peak global loads and global pressures during the event.

peaks (Määttanen, 1981), but this is not conclusive. In addition, if the total long-term ice exposure is to be considered, another factor to consider is the occurrence probability of low-speed events where the velocity effect may develop.

In Figure 8, the relation between ice exposure (in ice distance crushed) and high-speed loads and pressures for the events considered in this paper (Table 1) are shown. There are indications that more ice crushed during the highest-pressure events, but the longest event subverts this trend, and the trend is not visible for the loads. Note that the events with high mean loads are also the events with the highest peak loads, and vice versa for mean and peak pressures. That is, for the crushing events examined here, the factors contributing to a higher mean load and pressure during an event seems to have had a greater effect on the peak load and pressure rather than the event duration, or length of ice crushed.

Due to the difference in exposure dependence, comparing high-speed and low-speed maximum loads has little merit without having the actual distributions defined. In fact, the longer the duration of the high-speed measurement, the smaller the ratio between low-speed maximum and high-speed maximum is expected to become. Comparing low-speed maximum loads with high-speed mean loads as done in this work should also show variability depending on exposure. The variability is expected to be smaller assuming a narrower range of variation in peak loads with exposure observed for low speed and under the assumption that the effects of variability in ice properties average out. This may be the reason why we find a limited range (between 2 and 4) for this ratio in conditions of natural interaction (without a prepared ice edge). However, due to the lack of available data, the variability of the low-speed peak load to high-speed mean load ratio and how it is affected by different parameters such as exposure is ultimately unknown. As structural design is typically carried out by determining extreme-level and abnormal-level ice actions with associated annual probability of exceedance, further research should be carried out to determine how the low-speed peak loads vary with return period and exposure.

6. Conclusion

In this study, a method to account for the velocity effect in defining values for ice strength coefficients is explored. The method is used to estimate low-speed global peak loads and pressures for a structure at the location of the Norströmsgrund lighthouse in ice conditions encountered during the measurement campaigns between 1999 and 2003. The method is based on concepts rooted in model-scale and full-scale observations and at the basis of a numerical model for prediction of ice-induced vibrations that explains the velocity effect as a rapid 'strengthening' of ice at near-zero loading speed. The term 'strengthening' is being loosely used to define the effect of spatial pressure synchronization and/or improvement of contact between ice and structure resulting in an observed high global load. The framework suggests that the ratio of the maximum load that ice can exert on a structure at low drift speed to the mean load during high-speed brittle crushing has a relatively narrow range. Full-scale and model-scale data was found to suggest that this factor could be in the range of 3 to 4, depending mostly on the duration of low-speed loading and structural compliance. The load level which should be accounted for in design through an ice strength coefficient is thus connected with a certain state of the ice, which represents a shift in perspective from existing methods.

Applying the factor 3–4 times high-speed mean brittle crushing loads measured at the Norströmsgrund lighthouse shows that, for the time series analysed, a C_R value of 1.6 MPa used in Equation (2) gives an indication of the global pressures that could have developed for different ice thickness values given a very flexible structure at the same location and in the same ice conditions, or for sustained low speed loading on a rigid structure. The value of 1.6 MPa is somewhat lower than the value of 1.8 MPa specified for the Baltic Sea in ISO19906, the latter which may therefore be considered a safe value for design at the location of the lighthouse given the current state of knowledge. Note that due to the limited amount of data available, the occurrence probability of low-speed events and the exposure dependence of the associated peak pressures are unknown. Higher mean brittle crushing pressures

than those found in this work could potentially occur at the location, for example from naturally occurring higher ice strength not captured in the existing dataset. In that case a larger ice strength coefficient than 1.6 MPa would be needed to capture the corresponding low-speed events. Additionally, it was found that there is no singular way of estimating global pressures from the Norströmsgrund lighthouse data. Exact ice thickness values cannot uniquely be connected to peak panel loads in time, and the ice pressure estimation is sensitive to ice thickness variability, contributing to uncertainty in the estimation of low-speed peak global pressures.

Based on the analysis in this work, and the inherent uncertainties associated with the data from the Norströmsgrund lighthouse, it may not be safe to design structures in the Baltic Sea (for the ultimate or accidental limit states) for a nominal C_R representative of a 1-year maximum less than 0.9 MPa. This value would then reflect a synchronized interaction (three times the high-speed mean load) with a relatively weak ice floe as encountered at the Norströmsgrund lighthouse.

Notation

C_R	ice strength coefficient (Pa)
F_G	global load (N)
h	ice thickness (m)
P_G	global pressure (Pa)
w	structural width (m)

Acknowledgements

This paper is based on an earlier conference paper "Establishing the ice strength coefficient from mean crushing loads and a theoretical velocity effect", presented at the IAHR conference "27th IAHR International Symposium on Ice" in Gdańsk, Poland, 2024 (Hornnes et al., 2024). The authors wish to acknowledge the support to the FATICE project from the MarTERA partners, the Research Council of Norway (RCN), German Federal Ministry of Economic Affairs and Energy (BMWi), the European Union through European Union's Horizon 2020 research and innovation programme under grant agreement No 728053-MarTERA and the support of the FATICE partners. The authors thank the participating organizations in the SHIVER project: TU Delft and Siemens Gamesa Renewable Energy for supporting this work.

Disclosure statement

Vegard Hornnes declares employment by Equinor ASA, which may be considered a conflict of interest.

Funding

This work has been supported by the Norges Forskningsråd (NFR) sponsored project 326834: Risk of sea ice and icebergs for field development in the Southwestern Barents Sea (RareIce).

ORCID

Vegard Hornnes http://orcid.org/0009-0004-3537-2848
Hayo Hendrikse http://orcid.org/0000-0003-2252-4625

References

Bjerkås, M. (2006). *Ice action on offshore structures-with applications of continuous wavelet transforms on ice load signals* [Ph.D. thesis, NTNU], ISBN 82-471-7756-0.

Croasdale, K. (1977). *Ice engineering for offshore petroleum exploration in Canada*. Proc. 4th International Conference on Port and Ocean Engineering Under Arctic Conditions, St. John's, Canada.

Ervik, Å, Nord, T. S., Høyland, K. V., Samardzija, I., & Li, H. (2019). Ice-ridge interactions with the Norströmsgrund lighthouse: Global forces and interaction modes. *Cold Regions Science and Technology*, *158*, 195–220. doi:10.1016/j.coldregions.2018.08.020

Fransson, L. (2001). Development of ice load panels and installations at lighthouse Norstrømsgrund. LOLEIF Report No. 5-A.

Gagnon, R. E. (2012). An explanation for the Molikpaq May 12, 1986 event. *Cold Regions Science and Technology*, *82*, 75–93. doi:10.1016/j.coldregions.2012.05.009

Gravesen, H., & Kärnä, T. (2009). *Ice loads for offshore wind turbines in Southern Baltic Sea*. Proc. 20th International Conference on Port and Ocean Engineering Under Arctic Conditions, Luleå, Sweden.

Hendrikse, H., & Nord, T. (2019). Dynamic response of an offshore structure interacting with an ice floe failing in crushing. *Marine Structures*, *65*, 271–290. doi:10.1016/j.marstruc.2019.01.012

Hendrikse, H., & Owen, C. C. (2023). *Application of the suggested ice strength coefficients in ISO 19906 to intermittent crushing*. Proc. 27th International Conference on Port and Ocean Engineering Under Arctic Conditions, Glasgow, United Kingdom.

Hirayama, K., Schwarz, J., & Wu, H. (1973). *Model technique for the investigation of ice forces on structures*. Proc. 2nd International Conference on Port and Ocean Engineering Under Arctic Conditions, Reykjavik, Iceland.

Hornnes, V., Hendrikse, H., & Høyland, K. V. (2024). *Establishing the ice strength coefficient from mean crushing loads and a theoretical velocity effect*. Proc. 27th IAHR International Symposium on Ice, Gdańsk, Poland.

Hornnes, V., Høyland, K. V., Turner, J. D., Gedikli, E. D., & Bjerkås, M. (2020). *Combined distribution of ice thickness and speed based on local measurements at the Norströmsgrund lighthouse 2000-2003*. Proc. 25th IAHR International Symposium on Ice, Trondheim, Norway.

ISO19906. (2019). *Petroleum and natural gas industries – Arctic offshore structures*. International Organization for Standardization.

Kamesaki, K., Yamauchi, Y., & Kärnä, T. (1996). *Ice force as a function of structural compliance*. Proc. 13th IAHR International Symposium on Ice, Beijing, China.

Kärnä, T., & Masterson, D. M. (2011). *Data for crushing formula*. Proc. 21st International Conference on Port and Ocean Engineering Under Arctic Conditions, Montréal, Canada.

Kärnä, T., & Muhonen, A. (1990). Proc. 10th IAHR International Symposium on Ice, Helsinki, Finland.

Kärnä, T., & Qu, Y. (2006). Analysis of the size effect in ice crushing – edition 2. Version 1.3, 26-08-2009. VTT Internal report. RTE50-IR-6/2005.

Määttanen, M. (1981). Laboratory tests for dynamic ice-structure interaction. *Engineering Structures*, *3*(2), 111–116. doi:10.1016/0141-0296(81)90037-7

Nord, T. S., Samardžija, I., Hendrikse, H., Bjerkås, M., Høyland, K. V., & Li, H. (2018). Ice-induced vibrations of the Norströmsgrund lighthouse. *Cold Regions Science and Technology*, *155*, 237–251. doi:10.1016/j.coldregions.2018.08.005

Owen, C. C., Hammer, T. C., & Hendrikse, H. (2023). Peak loads during dynamic ice-structure interaction caused by rapid ice strengthening at near-zero relative velocity. *Cold Regions Science and Technology*, *211*, 103864. doi:10.1016/j.coldregions.2023.103864

Peyton, H. R. (1968). *Sea ice forces*. NRC of Canada, Technical Memorandum 92.

Schwarz, J., & Jochmann, P. (2001). *Ice force measurements within the LOLEIF project*. Proc. 16th International Conference on Port and Ocean Engineering Under Arctic Conditions, Ottawa, Canada.

Sodhi, D. S. (2001). Crushing failure during ice–structure interaction. *Engineering Fracture Mechanics*, *68*(17-18), 1889–1921. doi:10.1016/S0013-7944(01)00038-8

Sodhi, D. S., Takeuchi, T., Nakazawa, N., Akagawa, S., & Saeki, H. (1998). Medium-scale indentation tests on sea ice at various speeds. *Cold Regions Science and Technology*, *28*(3), 161–182. doi:10.1016/S0165-232X(98)00017-2

Thijssen, J., & Fuglem, M. (2015). *Methodology to evaluate sea ice loads for seasonal operations*. Proceedings of the ASME 2015 34th International Conference on Ocean, Offshore and Arctic Engineering, St. John's, Canada.

van den Berg, M., Owen, C. C., & Hendrikse, H. (2022). Experimental study on ice-structure interaction phenomena of vertically sided structures. *Cold Regions Science and Technology*, *201*, 103628. doi:10.1016/j.coldregions.2022.103628